

Beyond the Intelligent-shell Concept: the Clean-mode-control for Tearing Perturbations^{*)}

Paolo ZANCA

Consorzio RFX, Associazione Euratom-ENEA sulla Fusione, Padova, Italy

(Received 24 July 2008 / Accepted 29 January 2010)

The Intelligent Shell scheme, where a grid of active coils counteracts in a feedback scheme the measurements provided by an identical grid of sensors, has shown some limitations in the control of the dynamo tearing modes in RFX-mod. The origin of the problem is the aliasing on the measurements coming from the high periodicity sideband harmonics produced by the discrete nature of the active coils. A more efficient feedback on tearing modes is obtained by removing the sidebands from the measurements, thereby counteracting the true tearing Fourier modes. In this scheme, named Clean-Mode-Control, the sidebands are computed in real time from the coils currents using the cylindrical geometry approximation. The Clean-Mode-Control significantly alleviates the wall-locking of tearing modes in RFX-mod, giving the possibility of operating at a plasma current (1.5 MA) never reached before in a RFP machine. These features are well explained by a MHD model describing the tearing mode dynamic under the viscous torque due to the fluid motion and the electromagnetic torques produced by the feedback, the conductive structures surrounding the plasma and the non-linear interaction between the different modes [P. Zanca, *Plasma Phys. Control. Fusion* **51**, No. 1, 015006 (2009)]. Here some new results obtained with this model are discussed. In particular we will show that the edge radial field control improves by reducing the ratio between the delay introduced by the digital acquisition of the measurements and the time constant of the shell that contains the plasma. In this formulation the active coils are assumed to be located outside the shell.

© 2010 The Japan Society of Plasma Science and Nuclear Fusion Research

Keywords: dynamo tearing mode, proportional-derivative feedback controller, sideband, phase-locking, wall-locking, resistive shell

DOI: 10.1585/pfr.5.017

1. Introduction

In a magnetic confinement fusion device the presence of a conductive wall (shell) surrounding the plasma is important to guarantee a good magnetohydrodynamic (MHD) stability. However the finite penetration time of the radial magnetic field of any realistic shell determines potentially dangerous MHD phenomena, among which the wall locking of tearing modes (TM) [1, 2]. When the amplitude at the resonant surface is above the wall-locking threshold the mode is practically arrested in the laboratory frame and the stabilizing effect of the shell is lost: the TM radial field penetrates the shell and its amplitude considerably increases. Both in tokamaks and in reversed field pinches (RFP) this determines severe plasma-wall interactions and can lead to premature termination of the discharges. For example, in the RFX-mod reversed field pinch experiment [3] it is not possible to raise the plasma current above 500 kA and to have discharges lasting more than 150 ms, with the only stabilization provided by a shell whose characteristic penetration time, the shell time constant, is 0.1 s. However, we have to underline that the stabilizing effect of this shell on the TMs is reduced by the

presence of a far more resistive inner vacuum vessel (3 ms time constant), which decreases to very low amplitude the TMs wall-locking thresholds [2]. RFX-mod has demonstrated the possibility to overcome these limitations with the active control of the edge radial field, made possible by a grid of active coils, placed outside the shell, fully covering the torus. The first scheme tested, the so-called intelligent-shell (IS) [4], in which the coils are coupled in a feedback scheme with the measurements provided by an identical grid of radial field sensors, improves the plasma performances by preventing the radial field penetration of the shell [5]: besides a complete suppression of the resistive wall modes [6], the TMs edge amplitude is kept at a low value. In RFPs TMs in the non-linear regime are required by the dynamo mechanism in order to maintain the reversed configuration [7, 8]. Therefore these perturbations would exist even in the presence of a perfectly conducting shell. This means that, in general, a feedback system cannot suppress the non-linear dynamo TMs, but at the best it can keep to low values their edge amplitudes. A recent upgrade of the intelligent shell developed in RFX-mod, the clean-mode-control (CMC) [9, 10], leads to a better control of the TMs. In fact it fixes the TMs edge amplitudes at a lower level than the intelligent shell. Even more important, it maintains TMs into rotation for amplitudes at

author's e-mail: paolo.zanca@igi.cnr.it

*) This article is based on the invited talk at the 14th International Congress on Plasma Physics (ICPP 2008).

the resonant surfaces that are well above the wall-locking thresholds, while with the IS scheme TMs are observed to be always stationary in the laboratory frame. Even if these rotations occur at frequencies much smaller than the values related to the unperturbed fluid motion, they are enough to guarantee a good spread of the power deposition onto the first wall. The CMC is based on the real-time de-aliasing of the measurements from the high periodicity sidebands produced by the discrete nature of the active coils: the feedback variables are not the raw measurements, as in the intelligent shell, but the poloidal and toroidal m, n Fourier harmonics related to TMs, estimated as much correctly as possible with the sidebands subtraction. The basic effects of the CMC, namely TMs rotation and shell penetration avoidance are explained by a model solving the single fluid motion equation for several TMs at the same time, taking into account the viscous torque due to the fluid velocity and the electromagnetic torque developed by the interaction with the shell, the feedback currents and the non-linear interaction between different tearing modes [11]. This model can be viewed as a generalization to non-ideal boundary conditions, i.e. resistive shell and feedback, of the phase-locking code presented in reference [12]. Here we discuss some new results obtained with the model, which complete the analysis presented in [11].

2. The Clean Mode Control

To ease the discussion it is convenient to adopt cylindrical geometry with right-handed coordinates $(r, \theta, \phi \equiv z/R_0)$. We assume that the plasma, whose minor radius is $r = a$, is contained by a vacuum vessel modeled by a uniform resistive shell (the effects of gaps and holes are not considered in this analysis) of thickness δ_w , inner and outer radii respectively r_{wi} , $r_{we} = r_{wi} + \delta_w$. The shell time constant is defined by $\tau_w = \mu_0 r_{wi} \delta_w \sigma$, being σ the shell conductivity. The single shell configuration is the best case to investigate all the basic aspects of the problem. Outside the shell at the radius $r = c$ we have a grid of N_c -turn active coils, fully covering the torus. Both the active coils and radial field sensors, that we imagine to be placed at $r = r_{wi}$, are rectangles of poloidal and toroidal extent $\Delta\theta = 2\pi/M$ and $\Delta\phi = 2\pi/N$ respectively, centred at the angles $\theta_i = 2\pi/M \cdot (i - 1)$, $i = 1, \dots, M$, $\phi_j = 2\pi/N \cdot (j - 1)$, $j = 1, \dots, N$. The coil currents $I_{i,j}$ (= the total current in the i, j coil) and radial field measurements $b_{i,j}^r$ univocally define the set of discrete Fourier transform (DFT) harmonics $b_{r,DFT}^{m,n}$, $I_{DFT}^{m,n}$:

$$\begin{aligned} b_{r,DFT}^{m,n} &= \frac{1}{NM} \sum_{i=1,M} \sum_{j=1,N} b_{i,j}^r e^{-i(m\theta_i + n\phi_j)}, \\ I_{DFT}^{m,n} &= \frac{1}{NM} \sum_{i=1,M} \sum_{j=1,N} I_{i,j} e^{-i(m\theta_i + n\phi_j)}. \end{aligned} \quad (1)$$

Concerning the radial field, the Fourier modes are the physically relevant quantities, while in general the DFT harmonics are affected by the sidebands aliasing:

$$b_{r,DFT}^{m,n} = \sum_{\substack{p=m+LM \\ q=n+kN \\ (l,k) \in Z}} b_r^{p,q}(r_{wi}) f(p, q), \quad (2)$$

$$f(p, q) = \sin\left(q \frac{\Delta\phi}{2}\right) / \left(q \frac{\Delta\phi}{2}\right) \cdot \sin\left(p \frac{\Delta\theta}{2}\right) / \left(p \frac{\Delta\theta}{2}\right). \quad (3)$$

Due to their discrete nature, the active coils produce an infinite sequence of sidebands in the radial field, which enter in aliasing in expression (2):

$$b_r^{p,q}(r_{wi}, t) = \mathfrak{I}_{p,q} \cdot \int_0^t e^{A^{p,q}(t-\xi)} I_{DFT}^{m,n}(\xi) d\xi, \quad (4)$$

$$\mathfrak{I}_{p,q} = \mu_0 K_p' \left(\frac{|q| c}{R_0} \right) I_p' \left(\frac{|q| r_{wi}}{R_0} \right) \frac{q^2 c}{R_0^2} f(p, q) A^{p,q}, \quad (5)$$

$$A^{p,q} = \frac{1}{\tau_w} \left(p^2 / \left(\frac{q r_{wi}}{R_0} \right)^2 + 1 \right) / \left(K_p' \left(\frac{|q| r_{wi}}{R_0} \right) I_p' \left(\frac{|q| r_{wi}}{R_0} \right) \right).$$

Formulas (4,5) are the standard vacuum solution for the radial magnetic field in terms of the modified Bessel Functions I_p , K_p , with the shell penetration described by the thin-shell dispersion relation [9]. In fact if M, N are large enough, the sidebands do not correspond to any unstable plasma mode and they can be estimated from the coils currents using the vacuum approximation [9]. In the IS scheme the feedback variables are the measurements $b_{i,j}^r$:

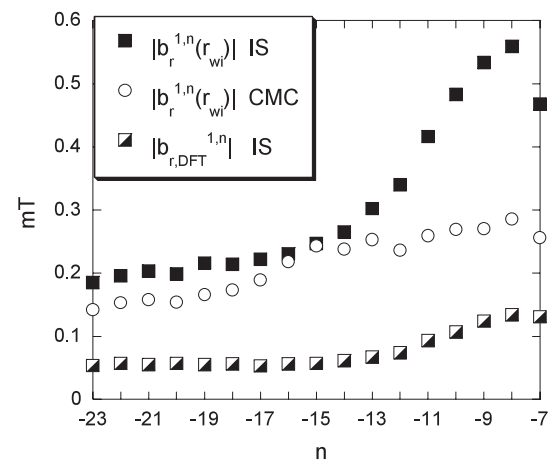


Fig. 1 Statistical analysis of the $m = 1$ TMs radial field amplitudes averaged between 20-200 ms for $I_p \approx 600$ kA shots in RFX-mod.

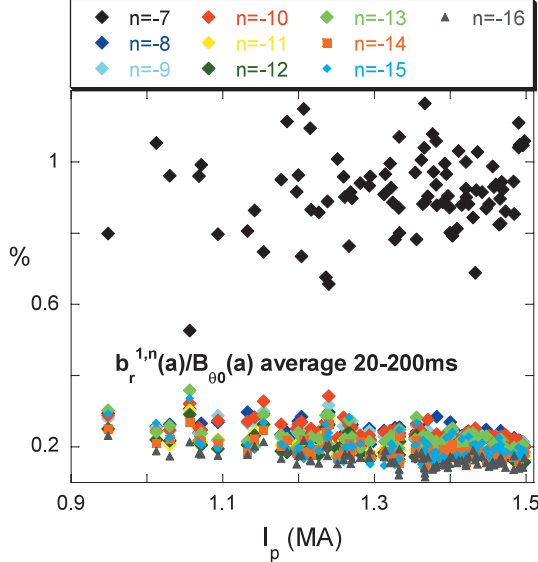


Fig. 2 Statistical analysis of the $m = 1$ TMs radial field normalized amplitudes. All the quantities are averaged between 20–200 ms

or equivalently the discrete harmonics $b_r^{m,n}$. Due to the aliasing effect this is not the best method to counteract the plasma perturbations. Instead in the CMC scheme the feedback variable are the Fourier modes $b_r^{m,n}$ related to the plasma perturbations: the sidebands $p \neq 0$, or $q \neq 0$ are computed in real-time from the coils currents using (4.5), and then subtracted in the expression (2) [9]. Of course, the aliasing effect in (2) can be reduced to negligible levels if the sensors and the active coils have very different periodicities in poloidal and toroidal directions. In this case the sidebands subtraction could not be necessary. As shown in Fig. 1, the IS control reduces the DFT harmonics of the measurements at a noise level (about 0.1 mT): the larger value observed for the Fourier mode amplitudes is a consequence of the sideband effect represented in formula (2). CMC indeed improves the control on the Fourier mode amplitudes. This figure considers the RFX-mode dynamo modes, which are the internally resonant $m = 1$, $n \leq -7$ TMs. A secondary branch of $m = 0$ modes with a large n spectrum resonating at the reversal surface ($q = 0$) is important for the non-linear interaction with the $m = 1$. The good edge amplitude control obtained with CMC produces a shrinking of the spectrum towards a quasi-single-helicity state (QSH), where we have a dominant mode, the innermost resonant $m = 1$ $n = -7$, and a tail of secondary modes ($m = 1$, $n < -8$). This is illustrated in Fig. 2, where the radial field is extrapolated at $r = a$ by combining the radial and toroidal field measurements available at $r = r_{wi}$ [9]. The QSH brings a reduction of the global plasma stochasticity [13]. As said in the introduction, while with the IS TMs are stationary in the laboratory frame, CMC maintains them into rotation. This is shown in Figs. 3(a), (b), where the radial displacement ξ_1 of the plasma surface due

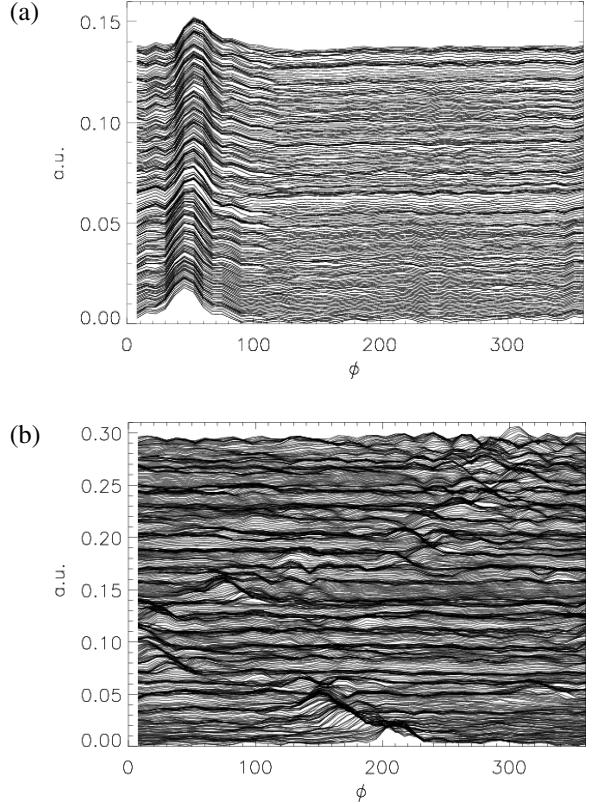


Fig. 3 (a) Waveforms of the plasma surface distortion $\xi_1(\phi)$ due to the $m = 1$ TMs, taken at different times. The displacement is computed adding the contributions of the $n = -1 \sim -23$ modes. Shot 18942 with IS. (b) Same quantities of (a) on the shot 22805 with CMC.

to the $m = 1$ TMs overlapping (obtained from the linear ideal-MHD Faraday-Ohm's law $b_r(a, \theta, \phi) = \mathbf{B}_0 \cdot \nabla \xi_r$, being \mathbf{B}_0 the equilibrium field) is plotted as function of the toroidal angle. Each curve represents a different time. In the IS case (a) we have a localized distortion, produced by the TMs phase-locking, which remains almost stationary in the laboratory frame; in the CMC case (b) the distortion moves around the torus and occasionally disappears. These movements are due to the fact that CMC maintains the individual TMs into rotation. Since the power deposition onto the first wall is associated to the localized distortion, the plasma-wall interaction is considerably mitigated with CMC. This beneficial effect, combined with the good control of the secondary modes amplitudes, allows reliable operations at 1.5 MA toroidal plasma current and discharge duration about 0.5 s [10].

3. Model Equations

The feedback effect on the dynamo TMs can be described by a model, explained in details in reference [11], considering the single fluid motion equation for the toroidal and poloidal flux-surface averaged angular velocities:

$$\rho \frac{\partial \Omega_\phi}{\partial t} = \frac{1}{r} \frac{\partial}{\partial r} \left(\mu r \frac{\partial}{\partial r} \Omega_\phi \right) + S_\phi \\ + \sum_{\substack{m \in \mathbb{Z} \\ n > 0}} \frac{\delta T_{\text{EM},\phi}^{m,n}}{4\pi^2 r R_0^3} \delta(r - r_{m,n}) = 0, \quad (6)$$

$$\rho \frac{\partial \Omega_\theta}{\partial t} = \frac{1}{r^3} \frac{\partial}{\partial r} \left(\mu r^3 \frac{\partial}{\partial r} \Omega_\theta \right) - \frac{\rho}{\tau_D} \Omega_\theta \\ + S_\theta + \sum_{\substack{m \in \mathbb{Z} \\ n > 0}} \frac{\delta T_{\text{EM},\theta}^{m,n}}{4\pi^2 r^3 R_0} \delta(r - r_{m,n}) = 0. \quad (7)$$

Here μ is the plasma perpendicular viscosity, ρ is the density, τ_D is the poloidal flow damping time and S_ϕ , S_θ are phenomenological steady momentum source densities which maintain the plasma rotation: for sake of simplicity we assume all these quantities to be constant with r . The vanishing of the velocities at $r = a$, and of their radial derivatives at $r = 0$ are taken as boundary conditions. The terms in the summation are the angular integrated electromagnetic torques, which develop in the proximity of the modes resonant surfaces ($q(r_{m,n}) = m/n$). They incorporate the contributions of the non-linear interaction between different TMs, the interactions with the image currents induced onto the shell and with the feedback coils currents. It is a standard result that the electromagnetic torque can be expressed by non-linear combination of the Newcomb's equation solutions for the TMs radial magnetic field perturbations (modes eigenfunctions) [2, 14]. The explicit expressions, valid when the plasma is surrounded by a resistive shell, are given in [11] (the zero-pressure condition is assumed for sake of simplicity). The Newcomb's solutions are everywhere continuous, but their radial derivative may have jumps across the resonant surfaces and the active coils radius (the active coil radial thickness is neglected). Moreover these solutions are not valid inside the shell region where another equation holds. Therefore, the Newcomb's solutions for each m, n TM are joined at $r = r_{\text{wi}}$ and $r = r_{\text{we}}$ with an equation derived in [15], describing the radial field diffusion inside the shell in the limit $\delta_w \ll r_{\text{wi}}$:

$$\tau_w \frac{\partial b_r^{m,n}}{\partial t} = \delta_w r_{\text{wi}} \frac{\partial^2 b_r^{m,n}}{\partial r^2}; \quad r \in [r_{\text{wi}}, r_{\text{we}}]. \quad (8)$$

Note that Eq. (8) is more general than the thin-shell dispersion relation [15], since it takes into account the radial field variation inside the shell. The radial field discontinuity at $r = c$ is related to the coils currents by the following relations obtained from the Ampere's law [16]:

$$\left. \frac{\partial b_r^{m,n}}{\partial r} \right|_{c-}^{c+} = -\mu_0 \left(\frac{m^2}{c^2} + \frac{n^2}{R_0^2} \right) f(m, n) I_{\text{DFT}}^{m,n}. \quad (9)$$

In this model, the current harmonics are provided by the following feedback equations:

$$\tau_d \frac{d}{dt} w_r^{m,n} + w_r^{m,n} = b_r^{m,n}(r_f, t), \quad (10)$$

$$I_{\text{ref}}^{m,n} = \frac{r_f}{\mu_0} \left(K_p^{m,n} w_r^{m,n} + K_d^{m,n} \frac{d}{dt} w_r^{m,n} \right), \quad (11)$$

$$V_{\text{DFT}}^{m,n} = \frac{R_c}{N_c} I_{\text{ref}}^{m,n}, \quad (12)$$

$$V_{\text{DFT}}^{m,n} = \frac{R_c}{N_c} I_{\text{DFT}}^{m,n} + l^{m,n} \frac{d I_{\text{DFT}}^{m,n}}{dt} + \lambda^{m,n} \frac{d b_r^{m,n}(r_{\text{we}})}{dt}. \quad (13)$$

In (10) $a \leq r_f \leq r_{\text{wi}}$ is the control radius (we assume that the radial field can be extrapolated in the entire vacuum region between plasma and shell as in RFX-mod), and dw_r/dt is the signal acquired by the feedback (w_r is obtained by integration). Equation (10) models the filter applied during the digital acquisition in order to avoid the aliasing in the frequency domain. The parameter τ_d could also include the delay due to the feedback operations such as the real-time Fourier analysis, if this delay is small in comparison with the TMs frequencies. We assume that the m, n Fourier harmonics can be correctly evaluated, with the removal of the coils produced sidebands as explained in Sect. 2. We will verify that this is indeed possible, which means that the sideband contribution to the measurements is not too large, at the end of Sect. 5. Equation (11) for the reference current harmonics represents the CMC law, here implemented as a standard proportional-derivative (PD) controller: $K_p^{m,n}$, $K_d^{m,n}$ are respectively the proportional and derivative gains applied to the m, n mode. Equation (12) is the discrete Fourier transform of the voltages $V_{i,j}$ applied to the coils, being R_c the resistance of the coil. Equation (13) is the RL circuital equation of the coils for the m, n current harmonics: $l^{m,n}$, $\lambda^{m,n}$ are effective inductances and areas respectively, whose explicit expressions are given in formulas (B.4), (B.5) of [11]. They provide the time variation of the radial flux enclosed by the coils. The inductances $l^{m,n}$ contain also the coils sidebands contribution. This is the only expression in which their effect is considered in this model: in fact, if M, N are large enough the sidebands do not correspond to unstable plasma modes and they are not expected to interact significantly with the TMs. The third term in the r.h.s of (13) is retained for sake of completeness, since its contribution is very small. Therefore the relationship between the reference and actual current harmonics, ensuing from (12, 13) is a one-pole filter law within a good approximation:

$$\tau_c^{m,n} d I_{\text{DFT}}^{m,n} / dt + I_{\text{DFT}}^{m,n} \approx I_{\text{ref}}^{m,n}; \quad \tau_c^{m,n} = l^{m,n} N_c / R_c. \quad (14)$$

Note that the pole inherits the m, n dependence of $l^{m,n}$. In [11] a slightly different formulation was adopted: Equation (14) was assumed to hold exactly with $\tau_c = 0.5$ ms, regardless to the mode numbers m, n , as observed in RFX-mod [17], and Eq. (13) was used to provide the voltages. In fact, in RFX-mod the coils amplifiers have an internal feedback system which from the one hand reduces the pole of (14), from the other hand introduces a fixed software delay: the consequence is that relation (14) is verified with $\tau_c = 0.5$ ms. In the present formulation we are not considering such a supplementary feedback system for

the coil amplifiers. In any case these are not important details, since the pole $\tau_c^{m,n}$ can be compensated by taking $K_d^{m,n} = \tau_c^{m,n} K_p^{m,n}$, which the analysis [11] indicated as the optimum choice for the derivative gain. In the computations shown in the next chapter the derivative gains are fixed according to this rule. The system of equations is closed providing the radial field at the resonant surface for each mode: we evolve the phases $\varphi^{m,n}$, while the amplitude are imposed, for example from the experimental estimates [18]. In fact the Rutherford-like models [19], which would provide equations for the amplitude evolution at the resonant surfaces in the non-linear regime are valid in single helicity conditions. Therefore, they are of uncertain applicability in the RFP case, where the observed dynamic involves the energy exchange between different TMs. The phases are assumed to evolve with the no-slip condition [1], according to which a tearing mode co-rotates with the ion fluid at the resonant surface:

$$\frac{d\varphi^{m,n}}{dt} = -n \Omega_\phi(r_{m,n}, t) - m \Omega_\theta(r_{m,n}, t). \quad (15)$$

4. Simulations

We take the fluid and equilibrium parameters from the RFX-mod experiment whenever possible, and fix them with sensible hypothesis in the absence of reliable determinations. The same geometrical dimensions and active coils grid of RFX-mod are assumed: $a = 0.459$ m, $R_0 = 2$ m, $c = 0.5815$ m, $M = 4$, $N = 48$, $N_c = 60$, $R_c = 0.8$ Ω. An important fluid parameter is the plasma perpendicular viscosity. To our knowledge, the viscosity in a RFP has been measured in MST only, perturbing the plasma velocity profile by a biased electrode [20]. From the flow damping, the perpendicular viscosity was inferred to be anomalous with a value $\mu/\rho \approx 50$ m²/s, which is assumed in these simulations. The imposed electron density is the value $n_e = 3 \times 10^{19}$ m⁻³ of the high current shot 23810 (1.5 MA), taken as reference. The poloidal damping time in Eq. (7) is taken equal to the viscous diffusion time: $\tau_D = \tau_V = \rho a^2/\mu$. The momentum sources in Eqs. (6), (7) are imposed in order to have, from the solution of the model equations, velocity profiles compatible with the RFX-mod measurements [21]. The fluid velocity is initialized to zero. The resistive shell is placed behind a non-conductive first wall made by graphite tiles: $r_{wi} = 0.475$ m (in RFX-mod the shell is placed farther from the plasma with respect to the simulation: $r_{wi} = 0.5125$ m). Moreover $\delta_w = 3$ mm as in RFX-mod. We will show some simulations examples considering the evolution of the $m = 1$, $n = -7 \sim -19$ modes non-linearly interacting with the $m = 0$, $n = 1 \sim 12$ modes. The amplitudes at the resonant surfaces are imposed according to the values estimated in the reference shot from the RFX-mod edge magnetic data using a Newcomb's equation solver [18]. Since we are considering a boundary different from the RFX-mod one, these amplitudes must be taken only as indicative of a high current RFP regime. These amplitudes are multiplied by an

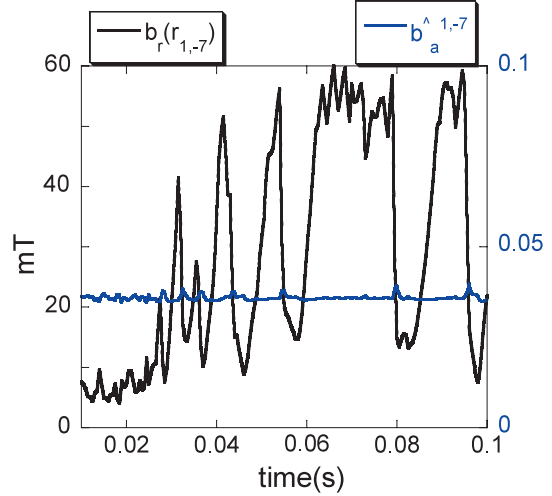


Fig. 4 Simulation result for the $m = 1$, $n = -7$ TM. Black: imposed amplitude at the resonant surface. Blue: merit parameter for this mode.

exponential factor to ensure the vanishing at the starting time of the simulation. The results of the analysis presented in [11] are summarized by the following points.

- 1) The transition from the high frequency rotation related to the unperturbed fluid motion to a slower frequency rotation is still present when the amplitude at the resonant surface exceeds the wall-locking threshold.
- 2) The feedback changes the properties of the slower branch, since the TMs frequencies remains significant and the shell penetration by the radial field is avoided.
- 3) At constant resonant surface amplitude, the feedback determines a true equilibrium condition, with uniform rotations; no signs of instability are seen unless the gains are increased too much.
- 4) The feedback does not fix the absolute value of the edge radial field, rather the ratio between the radial field at the plasma edge and at the resonant surface $\hat{b}_a^{m,n} \equiv |b_a^{m,n}(a)/b_r^{m,n}(r_{m,n})|$. We call this quantity the merit parameter. This is clearly show in Fig. 4, considering a simulation with $r_f = r_{wi}$ and $\tau_w = 0.1$ s. Despite the strong oscillations of the dominant mode amplitude at the resonant surface (characteristic of the QSH dynamic) the relative merit parameter remains almost constant.
- 5) Both $\hat{b}_a^{m,n}$ and the power $P_{i,j} = I_{i,j} \times V_{i,j}/N_c$ requested by the coils are reduced by increasing the shell time constant, until a saturation at about $\tau_w \approx 0.1$ s is found; from the one hand this means that the stabilization provided by the shell is important even with the feedback; from the other hand this implies that a thick shell with a very large τ_w is not necessary, and that the RFP can work with a relatively thin shell aided by the feedback coils
- 6) In the optimum range of τ_w and gains $K_p^{m,n}$ the values of $\hat{b}_a^{m,n}$ are slightly larger than those obtained with an ideal shell in the place of the resistive one.
- 7) Moving the control radius from the inner shell surface

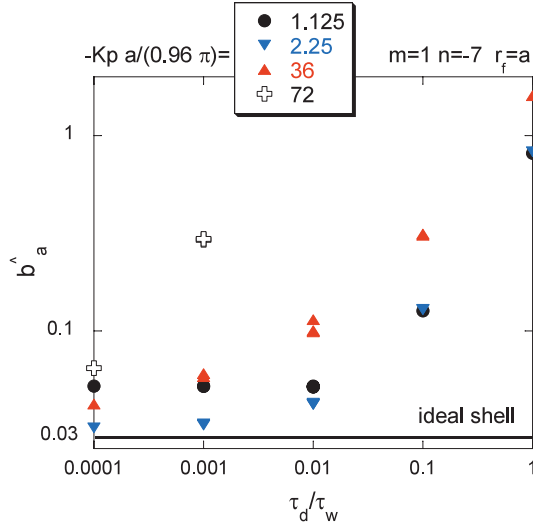


Fig. 5 Single mode analysis of the merit parameter $\hat{b}_a^{m,n}$ for the $m = 1, n = -7$ TM. The black line represents the value with an ideal shell in the place of the resistive one. Note the logarithmic scale in the y -axis.

$r_f = r_{wi}$ to the plasma edge $r_f = a$ does not improve the feedback performances in terms of $\hat{b}_a^{m,n}$ (they remain above the ideal shell values), while it increases considerably the power requested to the coils.

In all these analysis the parameter τ_d which enter in the ‘acquisition’ Eq. (10) was set at the value $\tau_d = 0.1$ ms. In the following we will present some complementary analysis, not published in [11], which consider a τ_d scan. Figure 5 shows the results of several simulation performed considering the $m = 1, n = -7$ TM only, assuming a constant amplitude at the resonant surface. The control radius is set at the plasma edge $r_f = a$. The points represent the $\hat{b}_a^{m,n}$ values once the equilibrium condition is established. For each of the nine combinations of τ_d, τ_w obtained with $\tau_d = (0.01, 0.1, 1)$ ms and $\tau_w = (0.001, 0.01, 0.1)$ s a $K_p^{m,n}$ scan is explored (the derivative gain is fixed by the condition $K_d^{m,n} = \tau_c^{m,n} K_p^{m,n}$). Values $\tau_w > 0.1$ s are not considered by virtue of the saturation effect mentioned at the point 5). Within a good approximation the merit parameter turns out to be a function of the gain and the ratio τ_d/τ_w . The values closest to the ideal shell one are obtain for small τ_d/τ_w and intermediate $K_p^{m,n}$. Raising the gain to much can lead to unstable solutions, as occurs for $-K_p^{m,n} a/(0.96\pi) = 72$ and $\tau_d/\tau_w \geq 0.01$, where in fact no points are shown. The τ_d/τ_w dependence is confirmed in the multi-mode simulations, with the ‘experimental’ imposed amplitudes at the resonant surfaces. In fact Fig. 6 shows a good agreement between the time-averaged $\hat{b}_a^{m,n}$ of two simulations having $r_f = a$, the same gains $K_p^{m,n}$, and the same ratio $\tau_d/\tau_w = 0.001$ obtained with two different combinations of τ_d, τ_w . The simulations are carried out for 10 ms with the ‘experimental’ amplitudes at the resonant surfaces taken in the interval [50, 60] ms (see black

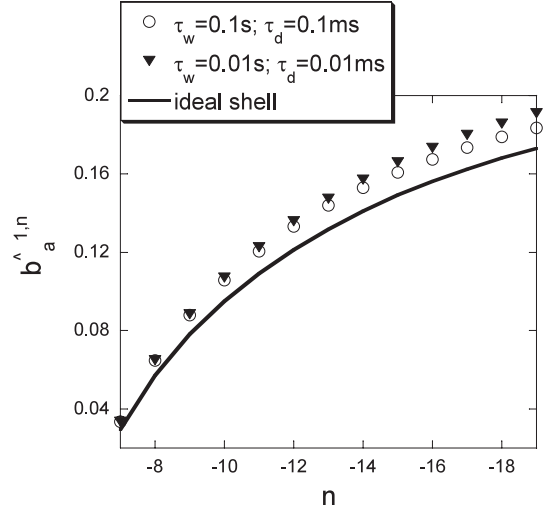


Fig. 6 Average values of for $\hat{b}_a^{m,n}$ the $m = 1$ TM in the multi-mode simulations with $r_f = a$ and $\tau_d/\tau_w = 0.001$. The black line represents the value with an ideal shell in the place of the resistive one.

line of Fig. 4). Therefore, the increase of $\hat{b}_a^{m,n}$ when reducing τ_w , obtained in [11] at fixed τ_d , can be compensated by a proportional reduction of τ_d . Nevertheless the simulation performed with the smallest τ_w is more demanding for the coils power, as shown in Fig. 7 by comparing the red and blue lines. The additional black line refers to a simulation performed moving the control radius at the inner surface of the shell $r_f = r_{wi}$: in this case the coils power is reduced. The coils power dependence on τ_w and r_f confirms the results of the previous analysis [11] mentioned at the points 5) and 7). In the inductances $I^{m,n}$ of Eq.(13) we have included the contribution of all the computable sidebands harmonics, while in [11] only the leading orders have been considered. This increases the computed voltages and consequently the coils estimated power in Fig. 7 by a factor 2-3 with respect to the analogous curves plotted in the figure 24 of [11].

As final analysis, we have verified the possibility of performing a CMC with the adopted configuration of coils, sensors and shell. This means that in the expression (2) for the DFT harmonics the ‘clean’ contribution, related to the Fourier modes $m = 1, n = -7 \sim -19$ and $m = 0, n = 1 \sim 12$, must be at least comparable to the sideband contribution. In fact if the latter were much larger than the former, the cleaning of the measurements with the sideband subtraction would be unfeasible, due to the unavoidable errors and approximations introduced by this procedure. Therefore in a post-processing of the simulation with $\tau_w = 0.1$ s and $r_f = r_{wi}$, the sidebands of the $m = 1, n = -7 \sim -19$ and $m = 0, n = 1 \sim 12$ TMs have been estimated from the coils currents using formulas (4, 5), and then added to the respective TMs harmonics according to (2) to obtain an estimate of the measured DFT

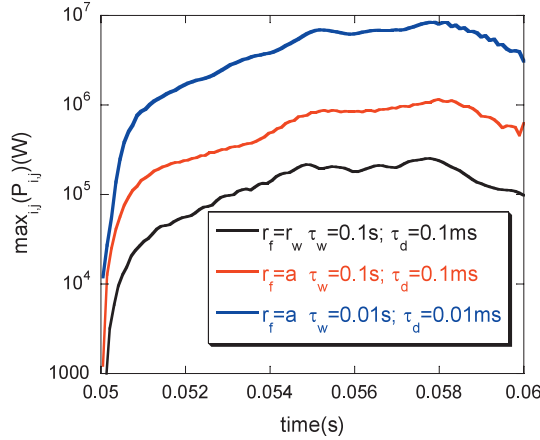


Fig. 7 Maximum of the coils power $P_{i,j} = I_{i,j} \times V_{i,j}/N_c$ as function of time for several simulations. The signals are smoothed for clarity reasons.

harmonics. The ‘raw’ signals $b_{i,j}^r$ are then given by the inverse of (1). The ‘clean’ part of the signals is instead obtained considering in the r.h.s of (2) the Fourier modes $m = 1, n = -7 \sim -19, m = 0, n = 1 \sim 12$ only, and then performing the same inverse transform of (1). Figure 8 compares the maximum of the 4×48 signals so obtained, showing that the clean contribution is a significant fraction of the total signal. The conclusion is that the CMC is indeed possible with the adopted layout. This is not surprising since this layout is similar to the RFX-mod one, where the CMC is currently used. We argue that the relatively large radial distance between sensors and coils (the sidebands decrease faster than the lower m, n harmonics of the TMs by increasing the distance from the coils) and the screening effect of the shell (the sensors are assumed to be placed on its inner surface) make the sideband contribution tolerable, despite the identical periodicity of sensors and coils.

5. Concluding Remarks

Some new aspects of the CMC feedback on the dynamo tearing modes with the active coils placed outside the vacuum vessel, assumed to be a uniform resistive shell, have been discussed. These results complete the general analysis presented in [11]. We have shown that the merit parameter $\hat{b}_a^{m,n}$ for the edge radial field control depends on the gains and on the ratio τ_d/τ_w between the time constants of the shell and of the filter necessary in the digital acquisition of the measured signals. Nonetheless τ_w should be large enough ($\tau_w \approx 0.1$ s) to reduce the coils power request, as already shown in [11]. The sidebands contribution to the measured signals has been estimated: for the assumed shell, sensors and coils layout (which is similar to RFX-mod) it remains at a tolerable level. The impossibility of reducing the merit parameter below the value obtained with an ideal shell in the place of the re-

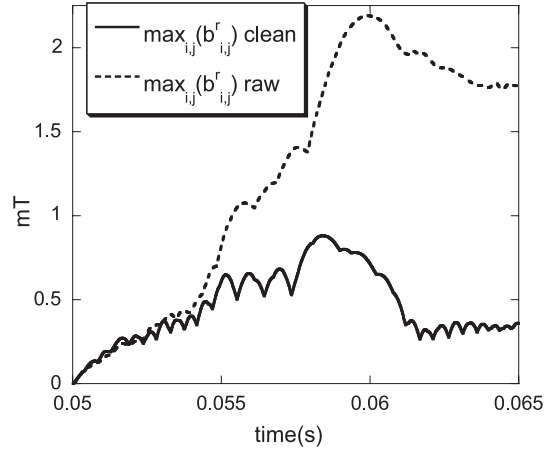


Fig. 8 Comparison of the raw and clean radial field measurements computed in a post-processing of the simulation with $\tau_w = 0.1$ s and $r_f = r_{wi}$. The sensors coils are at $r = r_{wi}$. Here the maximum of the $i = 1..4, j = 1..48$ signals is plotted as function of time.

sistive one, at least with a PD controller, is confirmed. The reason for this limitation is not easy to understand, since, for example, some analyses performed with more complex controller which cancels the non-linearities of the model equations (feedback-linearization technique [22]) suggest that, in the absence of delays, it is possible to make $\hat{b}_a^{m,n}$ close to zero. However, in these model-based controllers it is difficult to include a realistic description of the shell (the thin-shell dispersion relation was assumed in the place of the more exact Eq. (8)) Moreover the inclusion in the simulations of the delays related to the acquisition and coils amplifiers have shown to spoil the results. Perhaps it is better to consider the problem using a simpler argument, which from the one hand helps the intuition, form the other hand suggests a different feedback configuration. The best control of the edge radial field is realized when $\hat{b}_a^{m,n} = 0$, or equivalently $b_r(a) = 0$, since in this case the plasma would experience a ‘virtual’ ideal shell just at its boundary. If $b_r(a) = 0$ the external electromagnetic torque applied to the plasma is zero [11, 14], and TMs would rotate at frequencies close to their natural unperturbed values (apart a slight modification due to their mutual interaction [14]). At these frequencies the screening effect of the shell would make $b_r(r_{wi}) \approx 0$. Since Newcomb’s equation is a second order differential equation in r , these two conditions would imply the vanishing of the modes eigenfunctions, which is impossible. Instead, since the Newcomb’s solution is interrupted at the coils radius with a derivative discontinuity, the two conditions $b_r(a) = 0$, and $b_r(r_{wi}) \approx 0$ are compatible if the active coils are placed inside the vacuum vessel. An analysis of such a configuration, still in progress, is confirming this possibility.

[1] R. Fitzpatrick, Nucl. Fusion **33**, 1049 (1993).

- [2] R. Fitzpatrick *et al.*, Phys. Plasmas **6**, 3878 (1999).
- [3] P. Sonato *et al.*, Fusion Eng. Des. **66-68**, 161 (2003).
- [4] C.M. Bishop, Plasma Phys. Control. Fusion **31**, 1179 (1989).
- [5] S. Ortolani *et al.*, Plasma Phys. Control. Fusion **48**, B371 (2006).
- [6] B. Alper *et al.*, Plasma Phys. Control. Fusion **31**, 205 (1989).
- [7] C.G. Gimblett and M.L. Watkins, Proc. 7th European Conf. on Controlled Fusion and Plasma Physics, Lausanne, Vol.1, p.103, European Physical Society.
- [8] M.G. Rusbridge, Plasma Phys. Control. Fusion **33**, 1381 (1991).
- [9] P. Zanca *et al.*, Nucl. Fusion **47**, 1425 (2007).
- [10] L. Marrelli *et al.*, Plasma Phys. Control. Fusion **49**, B359 (2007).
- [11] P. Zanca, Plasma Phys. Control. Fusion **51**, No.1, 015006 (2009).
- [12] R. Fitzpatrick and P. Zanca, Phys. Plasmas **9**, 2707 (2002).
- [13] R. Lorenzini *et al.*, Phys. Rev. Lett. **101**, 025005 (2008).
- [14] R. Fitzpatrick, Phys. Plasmas **6**, 1168 (1999).
- [15] C.G. Gimblett, Nucl. Fusion **26**, 617 (1986).
- [16] R. Fitzpatrick and E.P. Yu, Phys. Plasmas **6**, 3536 (1999).
- [17] G. Marchiori, L. Marrelli *et al.*, ‘Advances in MHD-control in RFX-mod’, 35th EPS conference Hersonissos, Crete, Greece (2008).
- [18] P. Zanca and D. Terranova, Plasma Phys. Control. Fusion **46**, 1115 (2004).
- [19] N. Arcis, D.F. Escande and M. Ottaviani, Phys. Plasmas **14**, 032308-1 (2007).
- [20] A.F. Almagri *et al.*, Phys. Plasmas **5**, 3982 (1998).
- [21] L. Carraro *et al.*, Plasma Phys. Control. Fusion **40**, 1021 (1998).
- [22] H.J. Marquez, *Nonlinear Control Systems, Analysis and Design* (Wiley-Interscience, 2003).